DIRECT OBSERVATION AT A SHARP CRACK TIP VICINITY IN HYDROGENATED AUSTENITIC STAINLESS STEEL

Y. Katz,* H. Mathias* and S. Nadiv**

***Nuclear Research Center-Negev, Beer-Sheva, POB 9001, Israel**
****Technion Israel Institute of Technology, Haifa, Israel**

ABSTRACT

A combined study of localized effects caused by hydrogenation and austenite stability-degree aspects in 304L stainless steel was attempted. Localized events were investigated by plastic zone examination where stress-strain gradients prevail. On the other hand, austenite stability variations were included by tracking hydrogen influences at77°K and 298°K.

Due to the important role of hydrogen redistribution and release processes in activating phase transformation and microcracking, detailed approach was adopted, regarding possible controlling parameters. Specifically, the interrelationship between microstructural variables and hydrogen redistribution and release was focused.

Electrolytic charging was utilized on uniform and single edge notched (SEN) specimens. The plastic zone was formed by open mode loading before and after hydrogenation. Thermo-mechanical austenite stability, hydrogen induced martensitic transformation studies and microstructural mapping of the plastic zone were performed by x-ray diffraction and Mössbauer spectroscopy. Direct observations of hydrogen bubbles formation were performed and analized in the plastic enclave as well as at remote elastic regions.

Following the proposed experimental scheme, the overall view of dominating variables and their interaction in hydrogenated austenitic steels are discussed. Additionally few aspects related to cathodic charging parameters are further evaluated.

KEYWORDS

Austenitic stainless steels; hydrogen; cathodic charging, martensitic transformations; plastic zone.

INTRODUCTION

Hydrogen related effects, namely, plastic deformation, phase transformation and microcracking are influenced by metallurgical, environmental, geometrical and mechanical field variables. Austenitic stainless steels happened to be representative systems where hydrogenation induces phase transitions. Occasionally the

typical reaction of the form $\gamma \rightarrow \varepsilon' \rightarrow \alpha'$ has been experienced, (Holzworth and Louthan, 1968; Burke and others, 1972; Mathias and others, 1978) where ε' and α' are the hexagonal close-packed and the body-centered martensitic phases, respectively. Thus, austenite stability degree appears to be an additional parameter, calling for further research attention. Furthermore, if a stress-strain field is applied in such hydrogenated alloys, austenite decomposition occurs in the M_s-M_d range by plastic deformation and by internal hydrogen effects.

During the many years of extensive activity on hydrogen metal interactions and particularly topics related to hydrogen embrittlement, cathodic charging has been applied almost by routine fashion (Troiano, 1960; Smialowski, 1962). In fact, electrolytic charging was utilized in the current investigation with attempt to elaborate specific parameters directly relevant to this hydrogen charging technique. However, the main purpose of the present investigation lies in the combined problem of hydrogenation effects and austenite stability in frame of localized events study. Discussion concerning the importance of reduced scale observation, down to the microscale, has been already addressed elsewhere (Mathias and others, 1977). In this respect, the current study is actually an extension of previous experimental activities in a more detailed and refined approach.

Referring to hydrogen interactions in metastable austenite as occur in uniform and SEN specimens (specifically at the plastic zone), two main arguments are considered. Firstly, it is believed that only proper metallurgical definition of the plastic zone might promise progress in establishing the microstructural sensitivity to hydrogen interactions. Secondly, detailed investigation of hydrogen redistribution and release are in fact major issues, since these processes dominate and activate phase transformations and microcracking in austenitic stainless steels.

In order to illustrate the complexity of processes involved at the vicinity of a discontinuity, two different cases are described for identical electrolytic charging conditions. In one case the plastic-zone may consist of deformed almost monolithic γ . However, in case of low stability degree the plastic zone is a micro-multiphase structure, namely $\gamma + \varepsilon' + \alpha'$. Moreover, even if the initial microstructure after deformation is carefully controlled at the vicinity of the crack tip, hydrogen dynamic effects might alter it completely. This applies to plastic and elastic regions. As pointed out in previous studies (Mathias and others, 1977, 1978); austenitic steels as 304L, 316L and 310 result martensitic transformations due to hydrogenation even in the absence of applied stress field.

All these mentioned parameters and particularly structural variables, need to be accounted in the complex topics of hydrogen effects. Unfortunately very limited amount of quantitative information is available in the literature along this experimental field.

Keeping in mind the mentioned objectives, 304L was selected and uniform and SEN specimens were included. Direct observations of hydrogen bubble formation at the plastic and elastic regions were programmed with special attention to quantitative analysis and hydrogen redistribution. Additionally, examinations with a clear distinction between hydrogenation prior and after open mode loading of SEN specimens enabled further studies related to cathodic charging variables.

This proposed experimental scheme intended to crystallize a better physical view on hydrogen effects. The inclusion of austenite stability among other controlling parameters, might provide a more realistic description of possible hydrogen interactions and events in austenitic stainless steels.

EXPERIMENTAL PROCEDURES

Uniform and single edge notched tensile specimens were prepared from as-received AISI 304L stainless steel. The chemical composition is given in Table 1.

Table 1 Alloy Composition

Element	C	Cr	Ni	Mn	Mo	Si	Fe
Wt-%	0.03	18.2	10.7	1.7	0.5	0.48	bal

In order to eliminate undesired cold-work influences, spark-erosion was utilized for cutting and surfaces were electrolytically polished. Standard mechanical tests were performed at 298°K and 77°K. These included determinations of critical fracture toughness parameters. Prior to hydrogenation, the thermal and thermo-mechanical stability of the austenite γ - phase was studied, emphasizing the behaviour at ambient and cryogenic temperatures.

Temperature selection of 298°K and 77°K intended to introduce the variation of stability degree. Moreover, the detailed investigation in terms of localized events was achieved by plastic zones examination. The general scheme of the experimental procedure is summarized in Figure 1. Notice that hydrogenation before and after the developments of the plastic zone at constant strain rate was included.

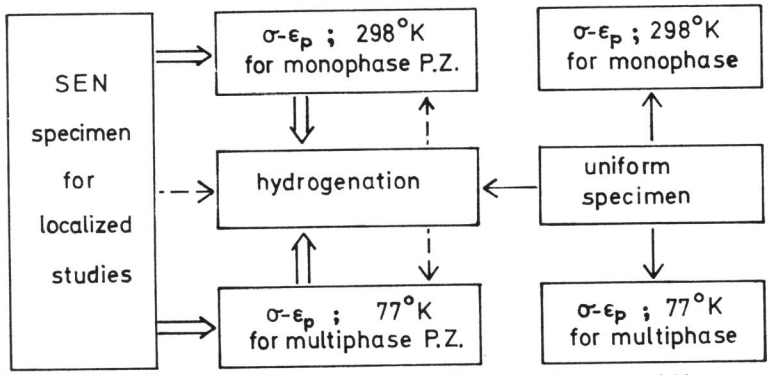

Fig.1. Scheme of experimental procedures. The specific arrows indicate the order of the experimental stages.

Hydrogen was introduced at room temperature into specimens by cathodic charging at a current density of 5 kAm^{-2}. The electrolytic cell was provided with a platinum anode and 1N H_2SO_4 electrolyte. 250mg arsenite per liter solution was added in order to delay hydrogen molecules formation.

Optical microscopy, x-ray diffractometry and Mössbauer transmission spectroscopy were applied. For the latter, a constant acceleration computerized spectrometer was used, utilizing a 25mCi $^{57}Co(Pd)$ source. Thin foils of appropriate thickness (5÷25μm) for the Mössbauer spectroscopy were prepared by electrolytic polishing.

X-ray diffractometry was mainly performed with the shallow penetrating CuKα radiation in steels. A graphite-monochromator was used in order to eliminate high fluorescence background. Radiations of higher penetrating power, namely CoK_α and MoK_α were used for comperative studies. This spread of radiation sources provided additional information, regarding especially proper phase concentration measurements.

To enable observation of effects which occur at very short time intervals after cathodic charging (Mathias and others, 1977; 1978), hydrogenated specimens were examined immediately after the charging termination. Here, X-ray diffractometry was repeatedly applied and continuous microscopic observation was performed. Additionally, the surface of hydrogenated specimen was covered with a glycerin layer. This enabled unique observation and analysis of released hydrogen bubbles formation and typical distributions. These observations were performed on specimens with applied constant strain-rate at ambient and cryogenic temperatures before and after hydrogenation, as shown in Fig.1.

EXPERIMENTAL RESULTS

Stress-strain curves for the selected material, are shown in Fig.2. As can be seen, the mechanical properties are strongly temperature dependent. At 77°K the steel revealed a considerably higher yield stress, strain hardening and fracture stress, but lower strain to fracture, than at ambient temperature. These differences are direct reflectionsof the thermo-mechanical instability of the austenitic γ-phase.

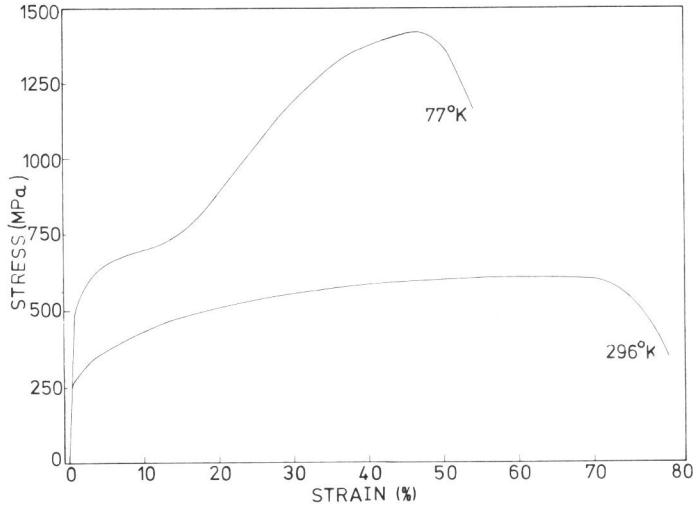

Fig.2. Engineering stress-strain curves for 304L stainless steel

As previously reported (Mathias and others 1977), the investigated 304L stainless steel showed high thermal stability, i.e. only monolithic γ-phase was observed even after immersion into liquid helium. External loading at 298°K resulted stable behaviour, and strain induced martensitic $\gamma \rightarrow \alpha'$ transformation occurred only at very high plastic strain. Cryogenic plastic straining resulted the well known $\gamma \rightarrow \varepsilon' \rightarrow \alpha'$ transformation sequence, when true plastic strains exceeded the value of 0.015.

Figure 3 illustrates typical results of the thermo-mechanical induced martensitic phase transitions for 304L SEN specimen strained at 77°K. Selected area x-ray diffraction was utilized in order to scan the plastic zone region (PZ) which developed during loading at the notch vicinity. This procedure was essential for the localized hydrogen effects, to be analized.

Figure 4 shows x-ray diffraction spectra for hydrogenated 304L stainless steel. While mechanically induced phases formed without delay, the hydrogen induced changes were time dependent. Especially, high-rate changes took place at very short times

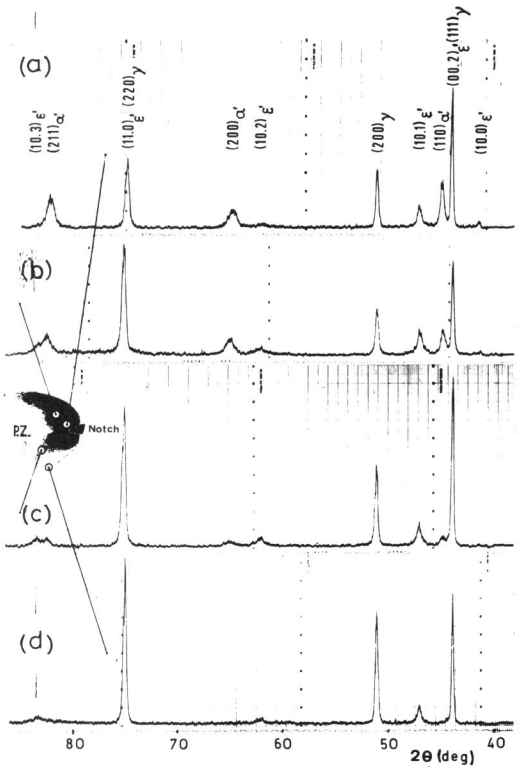

Fig.3. Selected area x-ray diffraction at PZ of unhydrogenated 304L SEN specimen. Straining temperature 77°K.

after hydrogenation. As clearly indicated in figure 4(a), every reflection peak of the γ-phase was accompannied by a second peak designated γ*. Repeated diffractometer scanning through 2θ angles revealed that γ* peaks moved continuously with time, until their position coincided with those of the original γ-phase (Fig. 4d). Similar position changes where observed for the reflection peaks designated ε* (Figs. 4a÷d). Accordingly, it was concluded that hydrogen induced γ* and ε* phases are actually expanded versions of the original γ and the martensitic ε'-phase respectively. Furthermore, it was observed that unexpanded martensitic α' formed in a delayed manner during the lattice contractions γ*→γ and ε*→ε'. At the same time the total amount of ε*+ε' decreased (Fig.4a÷d).

Quantitatively, x-ray spectra provided the determination of γ-products(volume or atomic fractions). In order to overcome difficulties due to preferred orientation, volume fractions Cϕ of the phases ϕ=α'; γ; ε', were calculated by extending the equation

$$C_\phi = K' \frac{V_\phi^2}{n_\phi} \sum_{\nu=1}^{n_\phi} \left(\frac{I_{hkl,\phi}}{F_T^2 . p . LP} \right)_\nu \qquad (1)$$

of Dickson's (1969) x-ray analysis to three phase materials, taking also reflection peak overlapping into account.

The factor K'was eliminated from Eq.1 by using the relation $\Sigma c_\phi = 1$. The unit volumes V_ϕ were calculated from d-spacing measurements. For every phase ϕ, the integrated intensities $I_{hkl,\phi}$, the multiplicity factors p, the Lorentz-polarisation factors LP and the structure factors F_T were determined for all n_ϕ reflections hkl of the scanned 2θ region. Calculations of the structure factors were based on the International Tables (1962; 1974), taking into account all transition elements of Table 1 and the corresponding Debye-Waller factors.

Phase concentrations were also determined from Mössbauer transmission spectra.Without entering into details of the quantitative procedure, some remarks are given. For specimens strained at 77°K or hydrogenated at 298°K, the Mössbauer spectra consisted of a central single paramagnetic peak (γ and ε'-phases) and six ferromagnetic hyperfine split peaks (α'-phase). The fraction of atoms present in the γ+ ε' phases and the α' phase were determined from area ratios of the corresponding Mössbauer absorption peaks.

Quantitative results obtained for uniform specimens, are given in Fig.5. Both, x-ray and Mössbauer data confirmed the sigmoidal shape of the α' phase. Typical increase of ε' up to 30% for 0.05 true plastic strain was obtained. Further straining resulted monotonic decrease of ε'.

Regarding the plastic zone (Fig.3), phase concentrations are listed in Table 2. As shown, the α'-phase and the ε'-phase are differently distributed over the plastic

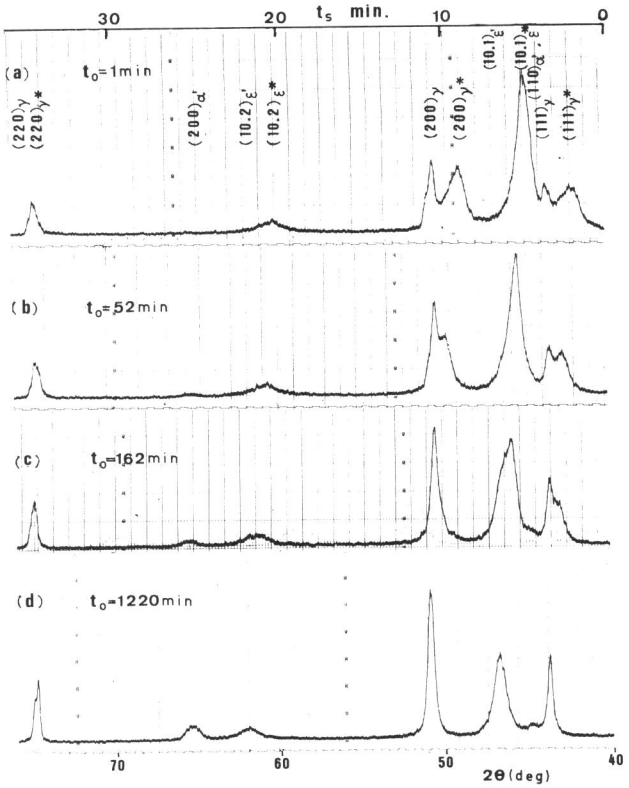

Fig.4. 304L x-ray diffraction patterns for time delays $t=t_s+t_o$ after hydrogenation of 120 min at 5 kAm^{-2}. t_s-time of spectrometer scanning, t_o-scanning start time after termination of hydrogenation.

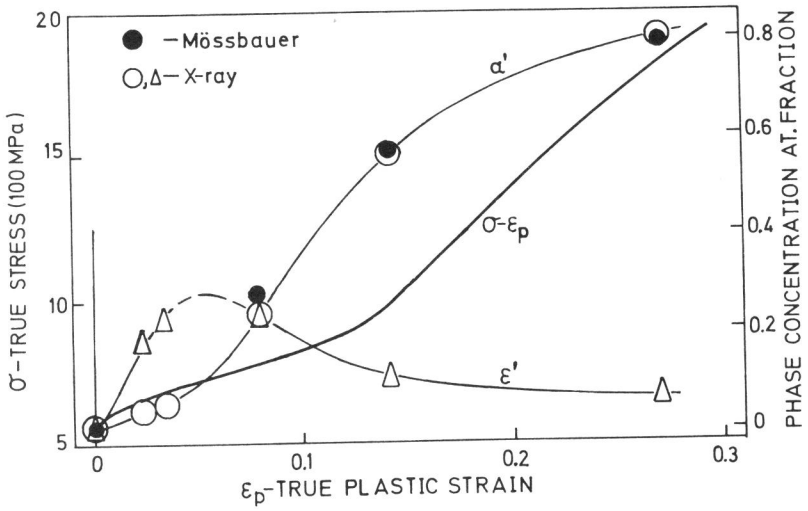

Fig.5. True stress-true plastic strain and corresponding phase concentrations for 304L uniform tensile specimens. Testing temperature 77°K.

zone region. In fact, highest α'-phase concentration was detected near the notch, where the plastic strains were largest. For different directions, the concentration of the α'-phase decreased with increasing distance from the notch. A relatively low ε'-phase concentration was obtained near the notch. However, near the elastic/plastic boundary, mainly ε'-phase was detected as γ-decomposition product, providing evidence that ε' is really an intermediate phase.

Table 2. Volume Fractions C_ϕ of Plastic Deformation or Hydrogen Induced Phases $\phi=\alpha'; \gamma; \varepsilon'$.

Volume fraction C_ϕ	After plastic deformation. Mapping according to indicated regions of Fig. 3 a	b	c	d	After hydrogenation
$C_{\alpha'}$	0.39	0.26	0.10	0.01	0.15
C_γ	0.45	0.51	0.70	0.81	0.62
$C_{\varepsilon'}$	0.16	0.23	0.20	0.18	0.23

For comparison, Table 2 includes results for hydrogenated specimens. Notice that α'- phase concentrations caused by normal hydrogenation resembled transformations due to true plastic straining of 0.065 at 77°K (Fig.5).

Microscopic observation of hydrogenated glycerin-covered specimens revealed that hydrogen evolved during several hours. Thus, hydrogen bubble dispersion micrographs, taken at different times, provided quantitative information. The volume $V(t_s)$ of hydrogen that emanated during time t_s from the unit area of a selected site was determined by :

$$V(t_s) = \frac{\pi}{6MS} \sum_i n_i D_i^3(t_s) \qquad (2)$$

Where; M - magnification factor, S - selected area and n_i - the number of bubbles with diameter $D_i(t_s)$ at time t_s.

In case of SEN specimens, straining at 298°K before hydrogenation indicated minor influences on early gas release rates. However, prolonged hydrogen emanation at PZ resulted significant preferential gas release. In fact, increase of about 30% of total evolved hydrogen was measured at the PZ relative to the elastic region. Straining at 77°K before hydrogenation showed similar behaviour, with one exeption, namely; accelerated hydrogen release during early stages at PZ.

During straining at 298°K of precharged specimens, enhanced hydrogen bubbles formation was observed. The effective area for the enhanced release matched completely the PZ while expanding as the latter increased to its final shape. Preferential release continued also after unloading. Figure 6a illustrates this behaviour. Similar tendencies, but much more pronounced effects were obtained for precharged SEN specimens strained at 77°K (Fig. 6b).

The effect of reloading was investigated at 298°K and 77°K. Generally, reloading resulted further increase of the preferential hydrogen emanation at the PZ. Figure 7a illustrates specific experimental variation. Here continuous hydrogen release from 298°K PZ (Fig.6a) was interrupted by cooling to 77°K and reloading at this temperature. Drastic changes, that occurred in hydrogen release behaviour, could not be attributed just to reloading effects. In fact, observations of continuous release, reloading effects and temperature transition effects provided the basis for proper comperative studies, Consequently, due to the intensified gas release at 77°K PZ, fast hydrogen exhaustion of the PZ resulted, as clearly emphasized in Fig. 7b.

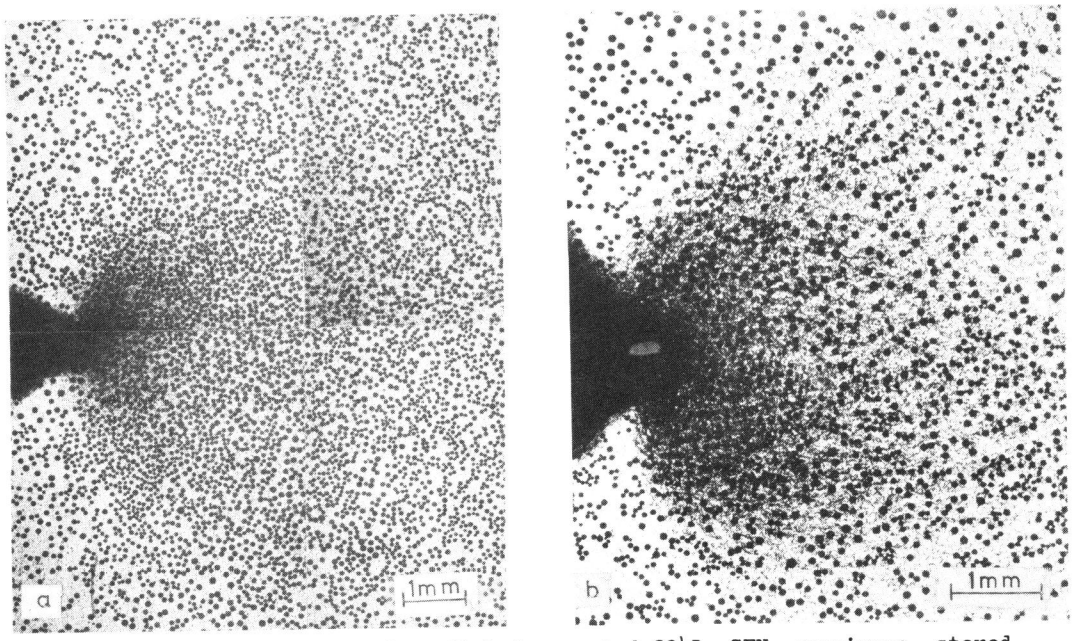

Fig.6. Hydrogen release from 2h hydrogenated 304L SEN specimens, stored 2h at 298°K and subsequently strained; (a) at 298°K with glycerin cover and examined 25min later: (b) at 77°K and glycerin covered after reheating to 298°K, examined 12min later.

Fractions $\eta(t_s)$ of hydrogen released from specific sites at the PZ relative to that released outside the PZ, were calculated on the basis of Eq.2, and are given in Table 3. Actually, this table demonstrates the possibility of refined PZ mapping in terms of preferred gas release, which should be compared to the already known plastic deformation induced martensitic phases formation as microstructural-background (Fig.3; Table 2).

Table 3. Volume Fractions $\eta(t_s)$ of Hydrogen Released During Time t_s at Sites $(\bar{r};\theta)$ of PZ Relative to Outside Regions.

Distance from crack tip r (mm)	Relative volume fractions $\eta(t_s)$ according to indicated Figures							
	Fig. 6a		Fig. 6b		Fig. 7a		Fig. 7b	
	$\theta=0^\circ$	$\theta=45^\circ$	$\theta=0^\circ$	$\theta=45^\circ$	$\theta=0^\circ$	$\theta=45^\circ$	$\theta=0^\circ$	$\theta=45^\circ$
0.3	2.7	2.9	3.3	3.7	5.8	6.5	0	0
0.5	2.3	2.7	2.4	4.0	4.4	6.2	0	0
0.8	2.2	2.4	1.8	2.9	3.7	5.3	0	0
1.0	2.1	2.2	1.7	1.8	3.2	4.6	0	0
1.5	1.9	2.1	1.3	1.5	2.9	4.3	0	0
2.0	1.9	2.2	1.5	1.4	2.6	3.5	0	0
3.0	1.8	2.1	1.4	1.6	2.4	3.0	0	0
4.0	1.5	1.7	1.2	1.4	2.2	2.5	0.6	0.4
6.0	1.2	1.4	1.1	1.2	2.1	1.8	0.8	0.8

Experimental results, as given for example in Tables 2 and 3 emphasize the role of microstructure variations and γ-stability in 304L on hydrogen effects. Hydrogen distribution and release processes are highly structurally sensitive. The reflection of these parameters, (as shown locally) on the sequential hydrogen effect, will be discussed later on.

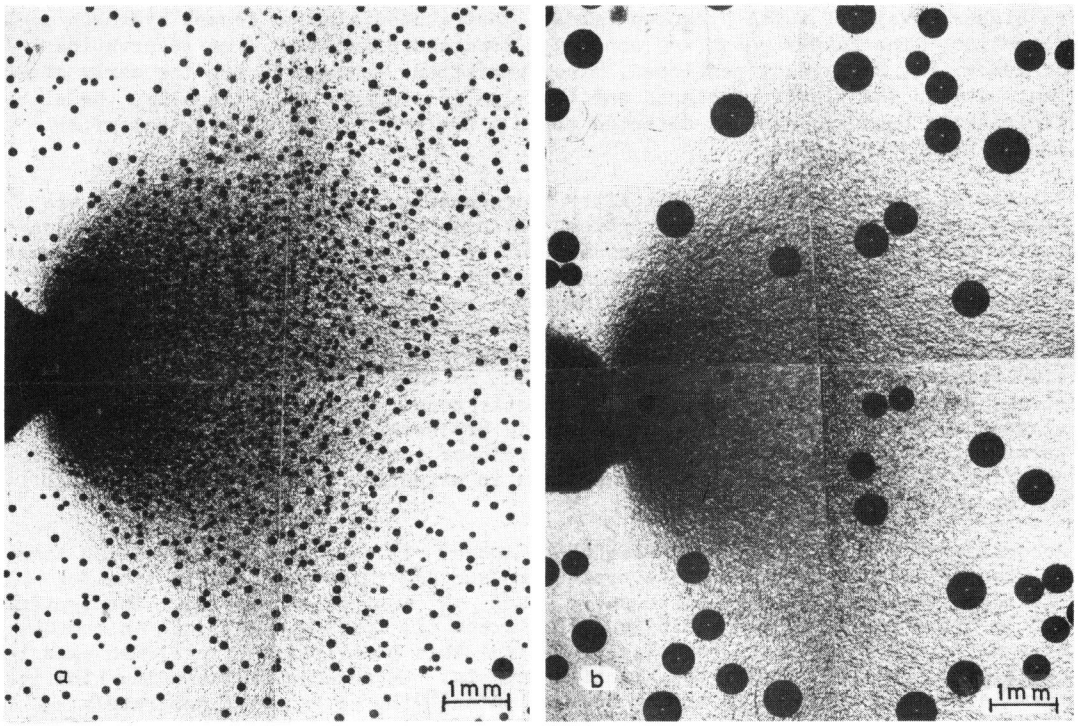

Fig.7. Hydrogen release from 304L SEN specimen shown in Fig,6a, reloaded at 77°K (2h after first straining) and reheated to 298°K. (a) subsequently glycerin covered and examined 1h later. (b) examined 18h after glycerin cover was renewed.

DISCUSSION

Referring to the experimental results, few points need some further explanation. Naturally the plastic zone size in specific material is controlled by the applied stress intensity factor. For open mode loading and for $\theta=0$; $x = r$, the plastic zone size r_p can be estimated by :

$$r_p = \frac{1}{\alpha}\left(\frac{K_I}{\sigma_y}\right)^2 \qquad (3)$$

Where; K_I - the applied intensity factor in open mode loading, σ_y - the yield stress of the nonhydrogenated or the hydrogenated material and α-constant dependent on the stress-strain state. Although the present results demonstrate mainly the localized reduced scale observations, the formation of a measurable plastic-zone satisfied the experimental demands. However, the complete data can be formulated in principle as a function of K_I serving as an independent parameter.

As shown, electrolytic hydrogenation after the PZ development indicated that the structure sensitivity of charging depends not only on austenite products due to plastic deformation (in case of 77°K PZ), but also on dislocation density, as shown in case of 298°K PZ. This finding confirms previous claims by Louthan and others (1972).

By analyzing the bubble dispersion vs. time, the role of the PZ is reflected mainly

in higher levels of total hydrogen release, attributed also to deeper hydrogen penetration. The latter point was concluded from short and long time observations of 298°K PZ. As already mentioned, minor variations occured during the early stages, between the plastic enclaved and the elastic regions. Additionally, the elastic/plastic boundary was not detected to be a preferential site, even not after long time observations.

In case of plastic zone formation after hydrogenation, the sequential events are summarized for a more lucid description. Deformation as such will cause accelerated hydrogen release as has been pointed out by Louthan and others (1972). However, the initial γ structure is preserved at ambient temperatures in the plastic zone, after short time delay. Notice that hydrogen release and redistribution with the absence of an external stress field induces delayed martensitic α' phase. On the other hand, deformation at low temperature transforms the material at the crack tip simultaneously. Thus, kind of superposition, or interactive nature of events will occur, as demonstrated in case of 77°K plastic zone. It has been the authors consistent approach that actually autocatalytic processes take place after charging termination. Hydrogen redistribution and release result transformations and microcracking, while both play significant roles in affecting further hydrogen redistribution and enhanced gas release.

Accordingly, kinetics arguments need to be added. If t_{obs} is the observation time, τ_d' is the delayed time for phase transformation and τ_d'' is the delayed time for microcracking, than t_{obs} relative to τ_d' and τ_d'' must be considered. The typical bubble distribution at the vicinity of the crack tip for $t_{obs} << \tau_d';\tau_d''$ is completely different than for $t_{obs} >> \tau_d';\tau_d''$. In fact this behaviour was confirmed experimentally, stressing clearly the kinetics aspects. Extended work including kinetics formulation and analysis is beeing carried on and will be reported separately.

Referring back to two important delayed events i.e. phase transformation and microcracking. Louthan and others (1972) utilized uniform specimen and monitored tritium release during uniaxial tension tests. Enhanced release was obtained in the plastic region and high peak at the fracture stage. Detailed observations in terms of hydrogen release near microcracks in hydrogenated specimens has been reported also by Katz and others (1977). Although the mentioned studies deal with relevant events, the role of structural parameters in stainless steels is far more involved.

The experimental programme included a wide range of t_{obs}, but the present experimental results emphasize examinations at $t_{obs} > \tau_d';\tau_d''$. This example was selected, since it demonstrates the main issues in more general fashion. Consequently, under the mentioned circumstances comparison between 298°K and 77°K plastic zones reflects influences with origins related to the initial microstructure and hydrogen related effects.

The stage of transition as shown in Fig.7a is particularly striking. The reloading at 77°K provided a sharp discontinuity in the gas release characteristics, indicating the structural sensitivity of hydrogen dispersion and release.

For the sake of a more complete picture, complementary information regarding fracture behaviour of 304L was recently obtained from parallel studies. The critical stress intensity factor of 130 MPa $m^{\frac{1}{2}}$ was measured at 77°K, compared to 85 MPa $m^{\frac{1}{2}}$ at 298°K. On the microscale, fractographic findings indicated that generally the ductile high energy mode still dominates at low temperature. Relative to the typical fracture mode at 298°K, some differences could be observed at low temperature, in terms of alternative fracture modes, mainly related to interphase decohesion. Clearly, the problem of microcracking or pre-microcracking, and therefore limitations due to variables isolation are recognized as major discussion points.

However, even by taking into account microcracking effects, the important role of plastic strain induced phases in hydrogen processes could not be masked. This conclusion is mainly based on detailed comparison between spatial distribution of the gas release and microstructure mapping illustrated for example in Table 3 and Figs.6 and 7. Further evidence supporting the structural sensitivity factor can be seen from data obtained at room temperature with applied loading and reloading.

At this stage comparison between Fig.6a and 7a can be more understandable. Actually in both cases the PZ contained induced martensitic phases. The PZ obtained at room temperature is bounded in terms of α'-phase level. On the other hand,phase concentration for the 77°K PZ is much higher as shown in Table 2. Consequently, volume fractions $\eta(t_s)$ of hydrogen release can be rationalized by the incorporation of α'-phase variations and by including carefully kinetics factors. In addition to the indicated tendencies, quantitative data provides proper basis for fundamental analysis.

As indicated, metallurgical parameters (austenite stability degree) and stress-strain field variables (plastic zone) are influencing hydrogen phenomena in stainless steel. Clearly, other secondary variables affecting γ decomposition and the plastic enclave might control local processes. Generally, proposed models have to recognize the involved physical situation. In this respect, the current contribution intends to add its share and assistance in building sound foundations along the mentioned research field.

CONCLUSIONS

1. Plastic zones can be microstructurally mapped and hydrogen effects can be tracked following the current proposed techniques. Consequently further investigation of the complex structural parameters becomes possible.

2. Comparison between 298°K and 77°K plastic zones in hydrogenated SEN specimens of 304L shows remarkable increase in hydrogen release rate. These variations are attributed to the induced martensitic phase transformations.

3. Hydrogen release and redistribution which locally activate phase transformations and microcracking are very structural sensitive in 304L stainless steel.

4. Austenite stability aspects should be defined and included in hydrogen-stainless steel interactions, for proper kinetics analysis and more complete view on controlling variables.

5. Deeper hydrogen penetration results at plastically deformed regions in hydrogenated 304L. Thus, cathodic charging depends on fine microstructure variables like dislocation density.

6. Generally, the elastic-plastic boundary is not dominating as preferential site of hydrogen uptake or release in 304L stainless steel.

ACKNOWLEDGEMENT

The authors wish to thank Mr. A. Bussiba and Mr. M. Kupiec of the Nuclear Research Centre, Negev, for experimental assistance during the current investigation.

REFERENCES

Burke, J., M. L. Mehta, and R. Narayan (1972). Hydrogen embrittlement of type 304L austenitic stainless steel. Cong. L'Hydrogene dans les Metaux, 1, pp. 149-158, Paris, Science et Industrie.

Dickson, M. J. (1969). The significance of texture parameters in phase analysis by x-ray diffraction. J. Appl. Cryst., 2, 176.

Holzworth, M. L., and M.R. Louthan (1968). Hydrogen induced phase transformations in type 304L stainless steels. Corrosion-NACE, 24, 110-124.

International Tables for X-Ray Crystallography (1962). Vol. 3, 235; (1974), Vol. 4, 72 & 149. The Kynoch Press, Birmingham, England.

Katz, Y., I. Shai, M. Lanxner, and H. Mathias (1977). Gas release from crystalline systems. 2eme Cong. Int. L'Hydrogene dans les Metaux, 7, 1F-8, Paris, Pergamon Press.

Louthan, M. R., G. R. Caskey, J. A. Donovan, and D. E. Rawl (1972). Hydrogen embrittlement of metals. Mater. Sci. Eng., 10, 357.

Mathias, H., Y. Katz, and S. Nadiv (1977). Post charging events in hydrogenated austenitic stainless steels. 2eme Cong. Int. L'Hydrogene dans les Metaux, 6, paper 2C-11, Pergamon Press.

Mathias, H., Y. Katz, and S. Nadiv (1978). Hydrogenation effects in austenitic steels with different stability characteristics. Metal Science, 12, 129-137.

Smialowski, M. (1962). Hydrogen in Steel, Reading, Mass. Addison-Wesley.

Troiano, A. R. (1960). The role of hydrogen and other interstitials in the mechanical behavior of metals. Trans. ASM, 52, 54.